

Direct observation of magnetic process in quasi-antiferromagnet by high resolution Kerr microscopy

Naoki Hashimoto¹, Shuu Horiike¹, Yuichiro Kurokawa¹, Po-Chun Chang², Wen-Chin Lin²,
Hiromi Yuasa¹

¹ Kyushu-Univ. ISSE
774 Motoooka Nishi-ku
Fukuoka 819-0395, Japan
Phone: +81-92-802-3706 E-mail: hashimoto@mag.kyushu-u.ac.jp

² National Taiwan Normal-Univ. Physics
88 Sec. 4, Ting-Chou Rd.,
Taipei116, Taiwan
Phone: +886-2-77346086 E-mail: wclin@ntnu.edu.tw

Abstract

We investigate a relationship between a magnetic hysteresis loop and domain structure modulation of a novel material, that is, a quasi-antiferromagnet (AFM) with domains of alternating antiparallel magnetization fabricated by a strong 90 deg magnetic coupling between two ferromagnetic layers through Fe-O thin layer. High resolution Kerr images exhibit the stripe type domains and magnetization mainly is along a longitudinal direction of domains throughout magnetization process, which indicates that the domain wall motion is dominant in the magnetization reversal of quasi-AFM. By fitting not only magnetization curve but also domain structure to LLG equation with 90 deg magnetic coupling energy, the 90 deg coupling coefficients were obtained properly, which makes possible to design the magnetic structure of quasi-AFM.

1. Introduction

Spin transfer torque (STT) in antiferromagnet (AFM) was theoretically [1-3] and experimentally [4-7] studied owing to the attractive properties, *i.e.*, THz frequency of spin torque oscillation (STO), no stray field, and so on. However, it is difficult to clearly observe STO in AFM because of strong exchange stiffness coupling between adjacent magnetic moments. Therefore, we fabricated quasi-AFM with domains of alternating antiparallel magnetization, resulting in a zero net magnetization by using 90 deg magnetic coupling [8-16]. The quasi-AFM exhibits FM coupling within one domain and AFM coupling between neighboring domains, which leads STO realization without stray field. We need to clarify and control the magnetic structure of the quasi-AFM because it is closely related with the magnetic dynamics. So far, we analyzed the quasi-AFM by scanning electron microscope with polarization analysis (SEMPA) and polarized neutron reflectometry (PNR) [17,18]. In contrast, the magnetic structure corresponding to magnetization process was not clear, although which is important for magnetic dynamic process. In this report, we observe magnetic domain motion

during magnetic process of quasi-AFM by using high resolution Kerr microscopy [19], and additionally explain the magnetic process quantitatively by comparing the Kerr images with simulated results.

2. Experiments and simulation model

Figure 1 shows a schematic image of sample structure sputtered on thermal-oxidized silicon. Since the magnetization of $\text{Co}_{90}\text{Fe}_{10}$ (A) is uniformly pinned by exchange coupling from IrMn and there is 90 deg magnetic coupling between $\text{Co}_{90}\text{Fe}_{10}$ (A) and $\text{Co}_{90}\text{Fe}_{10}$ (B) through Fe-O, $\text{Co}_{90}\text{Fe}_{10}$ (B) becomes a quasi-AFM. In order to obtain clear Kerr images, we used a capping layer of 1nm MgO. Magnetic field is applied from 10 mT to -10 mT in y -direction normal to pinning direction by IrMn. In the magnetic reversal, Kerr signals were measured at field increments of every 0.1 mT. Macroscopic magnetization process and domain motion were measured simultaneously.

In order to explain the domain motion quantitatively, we carried out Landau-Lifshitz-Gilbert (LLG) micromagnetic simulation by adding a 90 deg magnetic coupling term [20,21], $E = -A_{12}\mathbf{M}_1 \cdot \mathbf{M}_2 - B_{12}(\mathbf{M}_1 \cdot \mathbf{M}_2)^2$ where \mathbf{M}_1 and \mathbf{M}_2 are unit magnetization in the upper and lower layers, A_{12} and B_{12} are the bilinear and biquadratic coupling coefficients, respectively. The necessary conditions to realize the quasi-AFM are $|A_{12}| < 2|B_{12}|$ and $B_{12} < 0$. The probable values of A_{12} and B_{12} were estimated from fitting important to describe the magnetic dynamics of Quasi-AFM. The details are described in ref. [17]. By fitting the Kerr loop and images, the coefficients A_{12} and B_{12} were estimated.

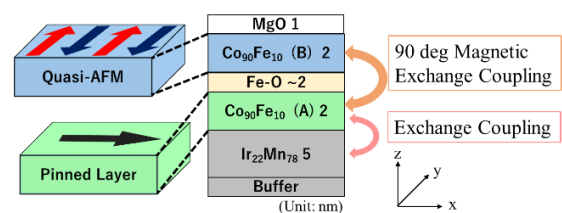


Fig. 1 Schematic image of sample structure and magnetization in pinned layer and quasi-AFM layer.

3. Results and Discussion

Figure 2(a) shows hysteresis loop measured by Magneto-optical Kerr effect. When the magnetic field is decreased from 10 mT to -10 mT, the magnetic domain was observed at the magnetic fields indicated as a - h and they are shown in Fig. 3 (a)-(h). Black and white indicates the magnetization directed toward the $+y$ and $-y$ direction, respectively. We can see the stripe domains in quasi-AFM with maintaining mostly $+/-y$ magnetization during the magnetization reversal. To be precise, there are two steps in the magnetic process. In the first step from 10 mT to zero, the average color of picture changes from white to grey, indicating the magnetic rotation. In the second step from zero to -2.8 mT, some tiny black regions with stripe shape appear and then grow, indicating the nuclei is main cause of the magnetic reversal. It is the first observation of the magnetic process in the quasi-AFM layers.

Below, we fit the above results to estimate the bilinear and biquadratic coupling coefficients A_{12} and B_{12} . Although A_{12} and B_{12} generally are estimated from the fitting of M - H curve, it has some ambiguity because an average of magnetization can be described by several series of A_{12} and B_{12} . Here, since we can refer the domain structure change to accurately determine A_{12} and B_{12} . Additionally, the variation of B_{12} was introduced in the calculation for describing the ununiform 90 deg magnetic coupling because the typical sputtered sample has roughness. As a result, when the set of $A_{12} = 0.4$ and $B_{12} = -0.2$ with the standard deviation of 0.12, the magnetization curve and domain motion were obtained as shown in Fig. 2 (b) and Fig. 3 (i)-(p). We can find the stripe domain with mostly $+/-y$ magnetization just like the Kerr images. The obtained coefficients of A_{12} and B_{12} are more proper than those estimated from magnetization curve alone. Such accurate coefficients are useful to design quasi-AFM domain size.

4. Conclusion

We succeeded to directly observe the magnetic process of quasi-AFM by means of high-resolution magneto-optical Kerr effect microscopy. It was revealed that there are two modes of magnetic reversal, magnetization rotation and nuclei growth. The nuclei grow to the stripe domain with mostly $+/-y$ magnetization, that is dominant in the magnetization reversal. The fitting to the domain motion leads the proper 90 deg magnetic coupling coefficients in LLG simulation, which would make possible to design of quasi-AFM domain structure.

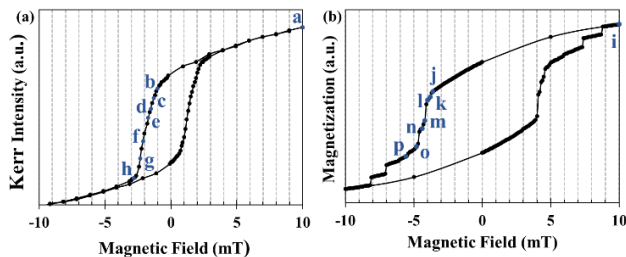


Fig. 2 Kerr signal hysteresis loop (a) and simulated magnetization curve (b) of quasi-AFM layer when a magnetic field H_y was swept.

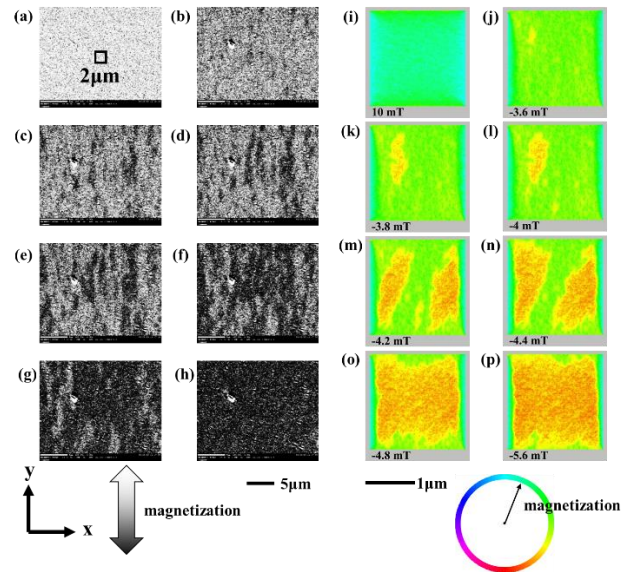


Fig. 3 Magnetic domain images in quasi-AFM layer measured by Kerr effect microscope (a)-(h) and simulated by LLG equation (i)-(p). Images of (a)-(p) correspond to points in Fig. 2.

Acknowledgements

This work was supported by JSPS KAKENHI (Grant No. JP19K04471).

References

- [1] A. H. MacDonald *et al.*, *Phil. Trans. R. Soc. A* **369** (2011) 3098.
- [2] A. S. Núñez *et al.*, *Phys. Rev. B* **73** (2006) 214426.
- [3] P. M. Haney *et al.*, *Phys. Rev. Lett.* **100** (2008) 196801.
- [4] Z. Wei *et al.*, *Rev. Lett.* **98** (2007) 116603.
- [5] S. Urazhdin *et al.*, *Phys. Rev. Lett.* **99** (2007) 046602.
- [6] Z. Wei *et al.*, *J. Appl. Phys.* **105** (2009) 07D108.
- [7] T. Moriyama *et al.*, *Appl. Phys. Lett.* **106** (2015) 162406.
- [8] J. C. Slonczewski, *Phys. Rev. Lett.* **67** (1991) 3172, *J. Magn. Magn. Mater.* **150** (1995) 13.
- [9] A. Fuss *et al.*, *J. Magn. Magn. Mater.* **103** (1992) L221.
- [10] C. J. Gutierrez *et al.*, *J. Magn. Magn. Mater.* **116** (1992) L305.
- [11] B. Heinrich *et al.*, *Phys. Rev. B* **47** (1993) 5077.
- [12] M. E. Filipkowski *et al.*, *Phys. Rev. Lett.* **75** (1995) 1847.
- [13] S. O. Demokritov, *J. Phys. D: Appl. Phys.* **31** (1998) 925.
- [14] P. A. A. van der Heijden *et al.*, *Phys. Rev. Lett.* **82** (1999) 1020.
- [15] H. Wang *et al.*, *Appl. Phys. Lett.* **90** (2007) 142510.
- [16] H. Fukuzawa *et al.*, *J. Appl. Phys.* **91** (2002) 6684.
- [17] G. Nagashima *et al.*, *J. Appl. Phys.* **126** (2019) 093901.
- [18] Y. Zhong *et al.*, *AIP Advances* **10** (2020) 015323.
- [19] P. Chang *et al.*, *Commun Chem* **2** (2019) 89.
- [20] M. Belmuguenai *et al.*, *Phys. Rev. B* **76** (2007) 104414.
- [21] S. Horiike *et al.*, *Jpn. J. Appl. Phys.* **59** (2020) SGGI02.